

Elsevier required licence: © <2021>. This manuscript version is made available under the CC-BY-NC-ND 4.0 license <http://creativecommons.org/licenses/by-nc-nd/4.0/>. The definitive publisher version is available online at [insert DOI]

Modeling and simulation of an extended ASM2d model for the treatment of wastewater under different COD: N ratio

Xinhui Zhang^a, Jun Nan^{a,*}, Tong Liu^a, Qiliang Xiao^a, Bohan Liu^a, Xu He^a, Huu Hao Ngo^b, An Ding^{a,*}

^a State Key Laboratory of Urban Water Resource and Environment (SKLUWRE), Harbin Institute of Technology, 73 Huanghe Road, Nangang District, Harbin, 150090, PR China

^b Faculty of Engineering, University of Technology Sydney, P.O. Box 123, Broadway, Sydney, NSW, 2007, Australia

* Corresponding authors.

E-mail addresses: nanjun0219@163.com (J. Nan), dinganhit@163.com (A. Ding).

Keywords:

Modeling

ASM2d

Wastewater

treatment Low

carbon source

EPS

SMP

A B S T R A C T

We evaluated the impact of chemical oxygen demand (COD) to nitrogen (N) ratios on the performance of a laboratory-scale anaerobic/anoxic/oxic (A²O) reactor by establishing an extended ASM2d model. This extended model introduced soluble microbial products (SMPs) and extracellular polymeric substances (EPS) to create the ASM2d-E-M. Other variables were introduced in the model to describe processes that already exist in the ASM2d, and those that were previously missing (e.g. EPS/SMP). To improve the accuracy of the simulation, this study included the establishment of the model, the division of model components, a sensitivity analysis, and model calibration and verification. The average errors of COD, ammonia and orthophosphate concentrations between the steady-state simulation data and experimental data, under different COD: N ratios were 7.42 %, 13.2 % and 9.18 %, respectively. Additionally, the average errors from the EPS and SMP simulation results were lower than 1.50 % and 2.59 %, respectively. The dynamic simulation results indicate that effluent COD, ammonia, orthophosphate and biopolymer concentrations decrease with an increase in influent COD: N ratio. But orthophosphate increases when COD: N increases to 16:1. Comparing the steady-state simulation and dynamic simulation of the model with the experimental procedure confirms that the model effectively describes the biological processes in an A²O reactor, accurately predicts SMP and EPS production in the activated sludge system under different COD: N ratios and provides a valuable tool for the operation.

1. Introduction

One of the challenges to the conventional process of biological nutrient removal (BNR) is insufficient organic carbon in influent [1]. When wastewater with a low carbon-to-nitrogen (COD: N) ratio is treated, effluent quality often does not reach a satisfactory level [2]. To overcome this, the anaerobic/anoxic/oxic (A²O) treatment process has become widely used in municipal wastewater treatment plants (WWTP) globally. This process has a number of advantages, such as an established design and operational practice, simple structure, short total hydraulic retention time, easy operational control, less sludge expansion, and the simultaneous removal of N and phosphorus (P) [3–5]. Recently, numerous methods aimed at the efficient exploitation of limited carbon sources have been developed for the A²O process to achieve high nutrient removal and efficient resource recovery from wastewater with a low C: N ratio [6].

The BNR of wastewater is a complex system involving physical, chemical and biological processes, in which all variables cannot be simulated individually through existing methods. The introduction of mathematical models into engineering practices, in conjunction with wastewater treatment simulation software, is important not only for design optimization, but also for improving the operation and control of BNR processes [7,8].

The International Association on Water Quality (IAWQ) activated sludge models (ASMs) represent an important breakthrough in the modelling of biological treatment processes. They are an efficient tool to design or assess WWTPs, while reducing operational costs [9,10]. ASM No. 1 (ASM1), which was developed to model biological oxygen demand (BOD) and nitrogen removal (NR), has become increasingly popular. However, it does not effectively describe the removal of all nutrients; therefore, ASM No. 2 (ASM2) was developed to incorporate the nutrient removal of N and P [11]. Resulting from this, ASM2d is a powerful tool,

based on the ASM2, which can be used to describe COD, N and P removals [12].

To improve effluent quality, many studies have focused on the properties of SMPs and EPS [13]. It is important to predict the ability of SMP and EPS in the activated sludge system because these materials can release secondary metabolites and as microbes, degrade pollutants in the BNR process. SMPs contain most of the soluble organic matter in wastewater from biological wastewater treatment plants [14]. In reaction processes, SMPs utilize most of the soluble O_2 , therefore dominating the COD [15]: their existence is particularly important for wastewater COD compliance. The presence of SMPs may, therefore, reduce the efficiency of the BNR. Furthermore, SMPs can cause issues, such as the formation of disinfection by-products, and the microbial growth of toxic substances [16]. Meanwhile, EPS content determines the microbial physiology, and the long-term stability of the sludge [17], as well as influencing its sedimentation and dehydration. Therefore, the accumulation of SMPs and EPS will significantly affect the performance of the bioreactor [17].

Although EPS and SMPs are produced during the activated sludge process, the current ASM2d does not include them in the model. To overcome this problem, and to define the removal of microbial nutrients more accurately, recent work has set out to improve the ASM2d. Marsili-Libelli et al. [18] proposed a new model that divides the nitrification stage into a two-step process, and includes improved phosphorus poly-microbials (X_{PAO}) dynamics for the anaerobic/aerobic P removal process. This model has the potential to simulate the actual conditions of a sewage plant as it overcomes some of the limitations imposed by the initial model. Rittmann et al. [19] has developed a unified theory that couples EPS and SMPs with active and inert biomass, and is able to reconcile apparent contradictions which treated EPS and SMP, as distinct entities. Jiang et al. [12] established an extended ASM2d, containing SMPs, and calibrated it on a laboratory-scale membrane bioreactor (MBR) system. This model can determine the best conditions for MBR operation. Yang et al. [20] has integrated soluble utilization associated products (S_{UAP}), soluble biomass-associated products (S_{BAP}) and extracellular polymeric substrates (X_{EPS}) into the ASM2d model, to create a new model which explores the mechanism and dynamics of SMP formation under different redox potentials. Experimental and modeling results have shown that biomass-associated products (BAPS) support a large number of SMPs, with high sensitivity to different redox potentials. This model was able to simultaneously minimize the excess sludge and increase the effluent quality. Yang et al. [21] also presented an extended ASM2 model, which was used to simulate and calibrate the role of EPS in the removal of P during anaerobic-aerobic processes.

So far, there have been few extended ASM2d models to simulate and

predict the A^2O process under different COD: N ratio conditions and SMP/EPS concentrations in the reactor. Therefore, an extended ASM2d-E-M model was developed by introducing two new components, S_{MP} and X_{EPS} , where S_{MP} represents soluble microbial products and X_{EPS} represents extracellular polymeric substrates. The ASM2d-E-M models the process of BNR, and the variation of SMP and EPS in the activated sludge process, as well as furthering our understanding of BNR at different COD: N ratios.

2. Materials and methods

2.1. Experimental setup and operation

Fig. 1 shows a schematic diagram of the A^2O process used in this study. The reactor was made of polymethyl methacrylate with a length of 0.96 m, a height of 0.35 m, a width of 0.33 m. It was divided into six compartments: an anaerobic zone (15.8 L), an anoxic zone (15.8 L) and four oxic zones (63.3 L). The reactors were operated at $20\text{ }^\circ\text{C} - 25\text{ }^\circ\text{C}$. The sludge retention time (SRT) was 15 days, while the mixed liquor suspended solids (MLSS) in the A^2O were controlled at $3200\text{ mg/L} - 3400\text{ mg/L}$ throughout the experiment. The flow rate for the returned sludge was 75 % and the internal recycling was 150 % of the influent flow rate. The total hydraulic retention time (HRT) was set at 12 h. Dissolved oxygen (DO) was controlled at $2\text{ mg/L} - 4\text{ mg/L}$ in the aerobic zones.

2.2. Characterization of the influent

All chemicals used were from Tianjin Fang Zheng Chemical Co. Ltd. (Tianjin, China). Starch, glucose (COD), ammonium chloride (NH_4Cl), urea, potassium dihydrogen phosphorus (KH_2PO_4), and sodium bicarbonate ($NaHCO_3$) were all analytical reagent grade. The influent wastewater was prepared using glucose and starch as the carbon source, NH_4Cl and urea as the nitrogen source, and KH_2PO_4 as the phosphorus source, along with trace elements. According to the design strategy, synthetic wastewater with different COD: N ratios (2:1 4:1, 8:1, 12:1 and 16:1) was fed into the reactor by adjusting the concentration of ammonium chloride in the inlet and used as model input. This provided a COD of $270\text{ mg/L} - 330\text{ mg/L}$, orthophosphate ($PO_4\text{-P}$) of $3.0\text{ mg/L} - 4.5\text{ mg/L}$ and ammonia nitrogen ($NH_4\text{-N}$) of $10\text{ mg/L} - 120\text{ mg/L}$, magnesium sulfate ($MgSO_4$) of 0.4 mg/L , calcium chloride ($CaCl$) of 6.0 mg/L , ferrous sulfate ($FeSO_4\cdot 7H_2O$) of 0.3 mg/L and other microelements, were added to the prepared sewage.

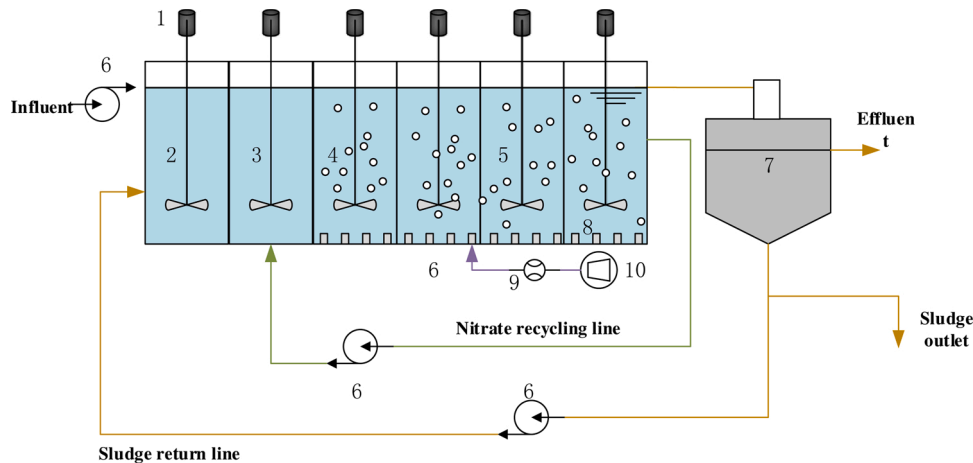


Fig. 1. Schematic diagram of A^2O : (1) Stirrer; (2) Anaerobic zone; (3) Anoxic zone; (4) Aerobic zone1; (5) Aerobic zone2,3,4; (6) Peristaltic pump; (7) Sedimentation tank; (8) Aerator; (9) Air flow-meter; (10) Air pump.

2.3. Analytical methods

The analyses of COD, total nitrogen (TN), NH₄-N (S_{NH}), total PO₄-P (S_{PO}) and MLSS were conducted following standard methods [22]. pH was measured with a pH meter (YSI pH10 Inc., USA), and DO concentrations were tested using a portable DO meter (HQ30D Inc., USA). Assuming that proteins (PN) and polysaccharides (PS) were the major components of SMP and EPS [12], the concentration of SMP was calculated using Eq. (1) proposed by Jiang et al. [12]:

$$SMP = (1.07 \times PS + 1.5 \times PN) / 0.64 \quad (1)$$

EPS content is the sum of PN and PS.

The concentration of PS was determined by the phenol-sulfuric acid method [23], with glucose as the standard, and PN quantification followed the improved Lowry method [24]. Prior to analyzing the EPS content, the sludge suspension was centrifuged at 8000 rpm for 5 min, then washed three times with deionized water. The supernatant was removed and the sample was added to 15 mL NaCl solution (0.05 %). The sludge mixture was placed in a water bath at 80 °C for 30 min, then centrifuged at 8000 rpm for 15 min. Finally, the supernatant was filtered through a 0.22 μm cellulose membrane and the extracted EPS was stored at 4 °C until analysis.

2.4. Parameter calibration and model evaluation

The parameter values for the conventional ASM2d, were obtained directly from [11,25]. The kinetic parameters and stoichiometry parameters used in the simulation program were based on the suggestions of the International Water Association (IWA) [26], as the initial model values. Process parameters, such as reactor volume and sludge reflux ratio etc. were simulated and input. A steady-state simulation, which ignores the influent changes over the operating period, was used in this test of the A²O system; the average influent data was calculated and simulated. A sensitivity analysis of the simulation results was carried out. In general, the analysis of parameter sensitivity can be divided into local sensitivity analysis and global sensitivity analysis. Selecting an appropriate method for sensitivity analysis is a compromise between the amount of information obtained from the analysis and the computational difficulty. A local sensitivity analysis means that the degree of sensitivity is determined through observing the influence of a small disturbance that is a local independent variable in the vicinity of the original parameter on the output value, as performed by Lu [27] and Jiang [28]. Whereas the global sensitivity analysis indicates that the parameter fluctuates within its value range, that is, the disturbance range is altered from local to global. This is demonstrated in the Extended Fourier Amplitude Sensitivity Testing (Extended-FAST) proposed by Cosenza [29] and the Standardized Regression Coefficients (SRC) method used by Mannina [30]. The global sensitivity analysis method is more expensive in terms of computation, and the interpretation of its result should be treated with caution. Since a plurality of parameters have been applied in the study, the local sensitivity analysis method is the most appropriate.

The kinetic parameters of the model gradually increased by 10 % from the initial value, while the other parameters remained constant. The parameters before and after simulation were compared, and the sensitivity of each parameter, regarding the effluent, was calculated according to Eq. (2):

$$\sigma_{j,i} = \frac{\frac{C_{i,1} - C_{i,0}}{C_{i,0}}}{\frac{\tau_{j,1} - \tau_{j,0}}{\tau_{j,0}}} = \frac{\frac{\Delta C_i}{C_{i,0}}}{\frac{\Delta \tau_j}{\tau_{j,0}}} \quad (2)$$

where $\tau_{j,0}$ is the initial value of the parameter; $\tau_{j,1}$ is the parameter value after the simulation; $C_{i,0}$ and $C_{i,1}$ are the concentrations of effluent before and after the parameter change. After an increase of 10 % from the initial values, the corresponding sensitivity values of parameters are

positive and negative points. A positive value indicates an increase in the parameter, which leads to increased effluent concentration. Based on the results of the sensitivity analysis, the most sensitive parameters were selected and optimized.

To evaluate the ASM2d-E-M, it was used to predict the effluent and biopolymer concentrations under different influent COD: N ratios. Then, the results of the model were compared with the experimental data to verify their accuracy.

3. Results and discussion

3.1. Model development

3.1.1. Model description

In this study, new components were introduced into the ASM2d model, proposed by Brun et al. [31], and it was extended to the ASM2d-E-M. The new parameters introduced are X_{EPS} and SMP. The extended model evaluated organic matter degradation in an activated sludge system, and the processes involved in the formation and degradation of EPS and SMPs. It was based on the Monod dynamics theory, to quantitatively describe the relationship between biological polymers and bacteria. Since the sensitivity analysis and calibration of the model will be more complicated with each additional parameter, the dynamics of parameter SMP in the ASM2d-E-M model is no longer traditional S_{BAP} and S_{UAP} [12], instead, it will be regarded as a whole as S_{MP}. This model also included a more comprehensive description of the mechanisms involved in the activated sludge system (including the interaction between heterotrophic organisms [X_H], autotrophic organisms [X_{AUT}] and phosphorus polymicrobials [X_{PAO}]), which can accurately simulate and predict the changes of water quality. Fig. 2 is the schematic representation of the metabolic process of BNR in the model.

3.1.2. Model kinetics

The kinetic model parameters and stoichiometric parameters of the extended ASM2d-E-M model are summarized in Table 1. As the remaining parameters are the same as the conventional ASM2d they are omitted here [32]. The kinetic rates expression (ρ_i) of the extended ASM2d-E-M model in the present work are shown in Table 2. Table 3 shows the stoichiometric coefficients (v_{ij}) of the extended ASM2d-E-M model.

In activated sludge systems, the concentration of a single component is affected by numerous different reaction processes. The advantage of the ASM matrix is that it can quickly and easily identify the changes of each component. The basic relationship for the balance of any given system in the ASM is (Input – Output + Reaction = Accumulation) [33]. The input and output terms are transmission phases, determined by the physical properties of the simulated system. The system reaction term, r_i , is obtained by calculating the sum of the product of the stoichiometric coefficient, v_{ij} , and the process rate formula, ρ_i , of component i , as shown in Eq. (3):

$$r_i = \sum v_{ij} \cdot \rho_j \quad (3)$$

By analyzing the role of SMP in biological growth, the kinetic rate expressions of aerobic and anoxic growth of X_H on SMP are as follows:

$$v_{SMP,NO} = \mu_{H,SMP} \eta_{NO_3,H} \frac{K_{O_2}}{K_{O_2} + S_{O_2}} \cdot \frac{S_{NO_3}}{S_{NO_3} + K_{NO_3}} \cdot \frac{S_{MP}}{S_{MP} + K_{SMP}} X_H \quad (4)$$

$$v_{SMP,O} = \mu_{H,SMP} \frac{S_{O_2}}{K_{O_2} + S_{O_2}} \cdot \frac{S_{MP}}{S_{MP} + K_{SMP}} X_H \quad (5)$$

As shown in Fig. 2, the growth of SMP is related to seven biological processes, including the decomposition of microbial cells to produce SMP and the hydrolysis of EPS. These processes are described by the Monod kinetic equation, and the kinetic rate equation. The growth of SMP is defined in Eq. (6):

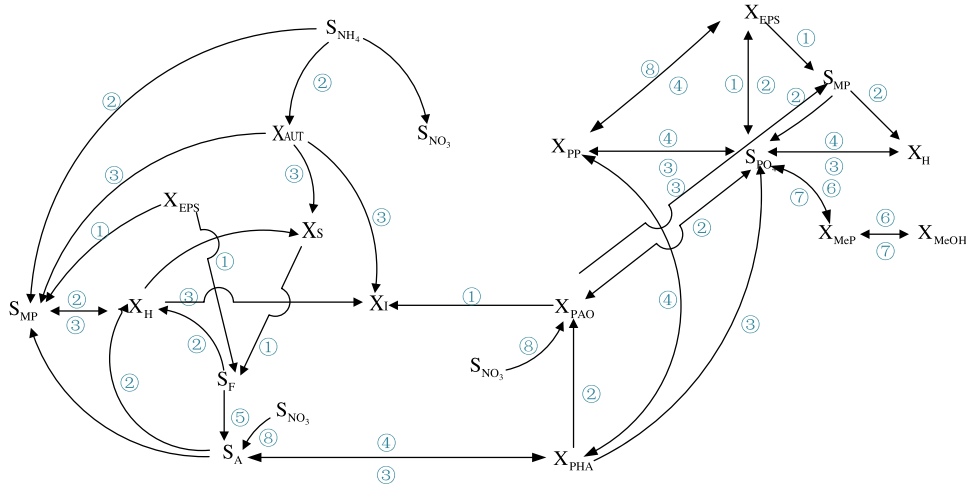


Fig. 2. Metabolic pathways of an ASM2d-E-M model: ① Hydrolysis; ② Growth; ③ Lysis; ④ Storage; ⑤ Fermentation; ⑥ Precipitation; ⑦ Redissolution; ⑧ Denitrification.

$$r_{S_{MP}} = \frac{f_{S_{MP,H}}}{Y_H} (\rho_1 + \rho_2 + \rho_3 + \rho_4) + (1 - f_{S_F}) (\rho_5 + \rho_6 + \rho_7) - \frac{1}{Y_{S_{MP,H}}} (\rho_8 + \rho_9) + \frac{f_{S_{MP,P}}}{Y_H} (\rho_{13} + \rho_{14}) + f_{S_{MP,L}} (\rho_{15} + \rho_{16} + \rho_{17}) - \frac{f_{S_{MP,A}}}{Y_A} \rho_{18} \quad (6)$$

The growth and reduction of EPS is related to the aerobic, anoxic and anaerobic growth of microorganisms. The kinetic rate equation of EPS is shown in Eq. (7):

$$r_{X_{EPS}} = \frac{f_{X_{EPS}}}{Y_H} (\rho_1 + \rho_2 + \rho_3 + \rho_4 + \rho_{13} + \rho_{14}) - (\rho_5 + \rho_6 + \rho_7) + f_{PP,EPS} (\rho_{11} + \rho_{12}) - \frac{f_{X_{EPS}}}{Y_A} \rho_{18} \quad (7)$$

3.2. Sensitivity analysis

To reduce the computational burden of the ASM2d-E-M, the initial values of ASM2d-E-M parameters are the default values of the conventional ASM2d. However, due to the introduction of many undefined new kinetic parameters and stoichiometric coefficients in the extended model, the values of these parameters will have a great impact on the rate of various biological processes in the model. This leads to a huge difference between the mode's prediction of the drainage volume and the actual measured data. The different influence of various parameters on water quality is also an important factor for parameter adjustment. Therefore, it is necessary to determine the newly added parameters according to the experimental data and parameter sensitivity analysis for the newly built extended model, so as to provide an accurate model for the simulation of BNR system. The sensitivity values are shown in Fig. 3.

It can be seen from Fig. 3 that parameters with high COD sensitivity include $f_{S_{MP,H}}$, $k_{h,EPS}$, k_{EPS} and Y_{PAO} . The highest sensitivity is seen in $f_{S_{MP,H}}$, with a maximum of 1.28, indicating that this parameter has the greatest impact on COD. The parameters with high sensitivity to S_{NH} are f_{SI} , Y_{PAO} , $i_{P,BM}$ and b_H . The four parameters with the highest sensitivity to phosphorous are q_{PP} , K_{PO_4} , b_{PAO} and $i_{P,X_{EPS}}$. The parameters with high sensitivity to X_{EPS} are $k_{h,EPS}$, k_{EPS} , μ_{PAO} , Y_{PO_4} and $\eta_{h,fe}$, and the parameters with high sensitivity to S_{MP} are $k_{h,EPS}$, $f_{S_{MP,H}}$, $\mu_{S_{MP}}$ and q_{PP} .

3.3. Parameter calibration

The parameter sensitivity distribution of a certain effluent index can be clearly defined using the analysis in Section 3.2. The work of this section was to make the simulated value more consistent with the

measured value by adjusting the higher parameters in the sensitivity distribution. To determine the parameters corresponding to SMP and EPS dynamics, a series of data is required. A range of data, i.e., COD, S_{PO} , S_{NH} , SMP and EPS concentrations, were collected from a laboratory-scale A²O operated under steady-state condition during a working cycle. Note that most of the parameters used in this paper are default values of ASM2d. Some parameters with low sensitivity were calibrated according to the method suggested by García et al. [34] or our previous research [2], or by referring to the calibrated parameter values. Parameters with high sensitivity were calculated using the stepwise calibration methodology proposed by Güçlü et al. [35]. The sensitivity parameter value was selected with a maximum output value changing by 25%. Specific calibration steps are shown in Fig. 4.

In addition, because the same parameter has an impact on two or more indexes in effluent COD, S_{NH} , S_{PO} , S_{MP} , and X_{EPS} of the model, these parameters must be adjusted repeatedly in the correction process. Therefore, special care needs to be taken in adjusting co-sensitivity parameters, and this should be avoided as much as possible.

Specific calibration steps are presented as follows:

Yields of X_H and X_{PAO} growth measured results are adjusted in accordance with the COD mass balance and steady-state simulation results, as well as the reference sensitivity analysis results. In the ASM2d-E-M, part of the influent substrates, CODs are directly applied in the SMP production, therefore, additional production of X_H and X_{PAO} from SMP is allowed. The S_{MP} score ($f_{S_{MP,H}}$) produced in the growth of X_H is set as 0.09, indicating that S_{MP} not only comes from the growth of biomass, but also generates other metabolic pathways [2], such as X_{EPS} hydrolysis, biomass attenuation and S_A degradation. Likewise, the value of Y_{PAO} is set as 0.61. At this point, the simulated COD value shows a good correlation with the measured value. As $k_{h,EPS}$ is also highly sensitive to X_{EPS} and S_{MP} , it is not adjusted temporarily for ensuring the parameter calibration effect of COD. The nitrification process is initially calibrated with only one parameter b_H ; however, such a calibration mode cannot fulfill fitting prediction for measured data. Hence, the value of $i_{P,BM}$ should also be gradually calibrated in successive iterations before measured data is accurately predicted. The phosphorus removal process is calibrated through adjusting highly sensitive parameters in the model. The predicted value of the model approaches the measured value when the sensitive parameters in the model: after adjusting, the q_{PP} value is 1.7. On this basis, K_{PO_4} and b_{PAO} are adjusted to 0.012 and 0.18, respectively. Parameters with high sensitivity to X_{EPS} are adjusted. k_{EPS} and μ_{PAO} are adjusted to 0.21 and 1.02, respectively, since the simulated value is greater than the measured value. Finally, parameters with high sensitivity to SMP are adjusted, as is the EPS hydrolysis rate constant,

Table 1

Stoichiometric and kinetic model parameters for the extended ASM2d-E-M model.

Parameters	Description	Value	Unit	References
$f_{SMP,H}$	Fraction of SMP produced during S_F growth on X_H	0.0963	$g\ S_{MP}/g\ X_H$	Jiang and Mynngheer [12]
$f_{X_{EPS}}$	Fraction of EPS produced during cell growth	0.12	$g\ X_{EPS}/g\ X_H$	Gao et al. [10]
f_{S_F}	Fraction of SF produced during EPS hydrolysis	0.4	$g\ S_F/g\ X_{EPS}$	Janus and Ulanicki [14]
$f_{PP,EPS}$	Fraction of EPS during X_{PP} storage and decomposing processes	0.1	$g\ S_{PO_4}/g\ X_{EPS}$	Yang et al. [20]
$f_{SMP,L}$	Fraction of SMP produced during cell lysis	0.0215	$g\ S_{MP}/g\ X_H$	(Jiang and Mynngheer [12]; Janus and Ulanicki [14])
$f_{SMP,A}$	Fraction of SMP produced during X_{AUT} growth	0.0963	$g\ S_{MP}/g\ X_H$	Jiang [12]
$\eta_{NO_3,H}$	Anoxic correction factor for Y_H growth	0.8	–	ASM2d
$\eta_{NO_3,PAO}$	Anoxic correction factor for Y_{PAO} growth	0.6	–	ASM2d
f_{SI}	Production of S_I in hydrolysis	0	$g\ COD/g\ COD$	ASM2d
f_{XI}	Fraction of inert COD generated in biomass lysis	0.1	$g\ COD/g\ COD$	ASM2d
Y_{PAO}	Yield coefficient (biomass/PHA)	0.625	$g\ COD/g\ COD$	ASM2d
Y_A	Yield of autotrophic biomass per $NO_3^- - N$	0.24	$g\ COD/g\ N$	ASM2d
Y_{PO_4}	PP requirement for storage of X_{PHA}	0.40	$g\ P/g\ COD$	ASM2d
Y_{PHA}	PHA requirement for X_{PP} storage	0.20	$g\ COD/g\ COD$	ASM2d
μ_H	Maximum growth rate of substrate	6.00	d^{-1}	ASM2d
μ_{PAO}	Maximum growth rate of PAO	1.00	d^{-1}	ASM2d
μ_{SMP}	Maximum rate of SMP degradation	0.0029	h^{-1}	(Ni and Zeng [6]; Yang et al. [20])
b_H	Rate constant for lysis and decay	0.40	d^{-1}	ASM2d
b_{PAO}	Decomposition rate constants of X_{PAO}	0.20	d^{-1}	ASM2d
b_{PP}	Decomposition rate constants of X_{PP}	0.20	d^{-1}	ASM2d
b_{PHA}	Decomposition rate constants of X_{PHA}	0.20	d^{-1}	ASM2d
q_{PP}	Rate constants of PP storage	1.50	d^{-1}	ASM2d
q_{PHA}	Rate constants of PHA storage (base X_{PP})	3.00	d^{-1}	ASM2d
$k_{h,EPS}$	EPS hydrolysis rate constant	0.0071	h^{-1}	(Ni and Zeng [6]; Yang et al. [20])
k_{EPS}	EPS formation coefficient	0.18	$g\ COD_{EPS}/g\ COD_S$	(Laspidou and Rittmann [44]; Ni and

Table 1 (continued)

Parameters	Description	Value	Unit	References
K_{O_2}	Saturation coefficient for oxygen	0.50	$g\ O_2/m^3$	Zeng [6]; Yang et al. [20]) ASM2d
K_{NO_3}	Nitrate affinity constant	0.50	$g\ N/m^3$	ASM2d
K_A	S_A affinity constant for heterotroph	4.00	$g\ COD/m^3$	ASM2d
K_{PO_4}	Saturation coefficient for phosphate	0.01	$g\ P/m^3$	ASM2d
K_{ALK}	Alkalinity affinity constant for heterotroph	0.10	$mol(HCO_3^-)/m^3$	ASM2d
K_{SMP}	Biomass affinity constant for SMP	85	$g\ COD_{SMP}/m^3$	(Laspidou and Rittmann [44]; Ni and Zeng [6]; Yang et al. [20]) ASM2d
$\eta_{h,fe}$	Anaerobic correction factor for X_{EPS} hydrolysis	0.4	–	ASM2d
$i_{P,BM}$	P contents in X_H , X_{PAO} , X_{AUT}	0.02	$g\ P/g\ COD$	ASM2d
$i_{P,X_{EPS}}$	P contents in X_{EPS}	0.02	$g\ P/g\ COD$	ASM2d
$i_{P,SMP}$	P contents in SMP	0.02	$g\ P/g\ COD$	(Jiang [12])
f_{SMP}	Fraction of S_F produced during X_{EPS} hydrolysis	0.4	$g\ S_{MP}/g\ X_{EPS}$	(Janus and Ulanicki [14])
$f_{PP,EPS}$	Fraction of EPS during X_{PP} storage and decomposing processes	0.1	$g\ S_{PO_4}/g\ X_{EPS}$	Yang et al. [20]
$Y_{H,SMP}$	Yield coefficient for growth on SMP	0.45	$g\ COD_x/g\ COD_{SMP}$	(Laspidou and Rittmann [44]; Ni and Zeng [6]; Yang et al. [20])
$f_{SMP,P}$	Fraction of SMP produced during X_{PAO} growth on PAO	0.0963	$g\ S_{MP}/g\ X_H$	Jiang [12]
Y_H	Heterotrophic yield coefficient	0.625	$g\ COD/g\ COD$	ASM2d

$k_{h,EPS}$. After that, the altered COD value is greater than the previously-calibrated value. Consequently, a secondary adjustment is conducted on COD. The above steps, with $f_{SMP,H}$ adjusted to 0.08, are repeated until the predicted COD value is consistent with the measured value. Meanwhile, the predicted value of X_{EPS} is also altered. In this case, the k_{EPS} value is adjusted to 0.24 and then to 0.003 and the value in the previous step is adopted as the value of q_{PP} without adjustment, since the predicted value of S_{MP} agrees with the measured value, and the adjustment of q_{PP} might exert an influence on the value of S_{PO_4} . This can then be applied to dynamic data (obtained from measurement activities) within the period. Table 4 presents the calibrated results of these nine model parameters.

3.4. Model verification: simulation of the BNR system

3.4.1. Nutrient removal and model verification performance

The purpose of this section is to verify the ASM2d-E-M model by comparing the simulation results with the measurement results of pollutants along the A²O reactor in each cycle under different COD: N ratios. If the average error between the calculated value of the predicted result and the measurement result is within 50 %, then the result is considered acceptable. Fig. 4 shows the steady-state detailed performance of COD, N and P removal rate and SMP, EPS concentrations at

Table 2

Kinetic rates expressions in the extended ASM2d-E-M model.

Process	ρ_i
1 Aerobic growth of $X_{H\text{ on } S_F}$	$\mu_H \frac{S_{O_2}}{K_{O_2} + S_{O_2}} \frac{S_F}{S_A + S_F} \frac{S_F}{S_F + K_F} \frac{S_{NH_4}}{S_{NH_4} + K_{NH_4}} \frac{S_{PO_4}}{S_{PO_4} + K_{PO_4}} \frac{S_{ALK}}{S_{ALK} + K_{ALK}} \cdot X_H$
2 Anoxic growth of $X_{H\text{ on } S_F}$	$\mu_H \eta_{NO_3, H} \frac{S_{O_2}}{K_{O_2} + S_{O_2}} \frac{S_A + S_F}{S_A} \frac{S_F + K_F}{S_F} \frac{S_{NH_4}}{S_{NH_4} + K_{NH_4}} \frac{S_{NO_3}}{S_{NO_3} + K_{NO_3}} \frac{S_{PO_4}}{S_{PO_4} + K_{PO_4}} \frac{S_{ALK}}{S_{ALK} + K_{ALK}} \cdot X_H$
3 Aerobic growth of $X_{H\text{ on } S_A}$	$\mu_H \frac{S_{O_2}}{K_{O_2} + S_{O_2}} \frac{S_A + S_F}{S_A} \frac{S_F + K_F}{S_F} \frac{S_{NO_3}}{S_{NO_3} + K_{NO_3}} \frac{S_{NH_4}}{S_{NH_4} + K_{NH_4}} \frac{S_{PO_4}}{S_{PO_4} + K_{PO_4}} \frac{S_{ALK}}{S_{ALK} + K_{ALK}} \cdot X_H$
4 Anoxic growth of $X_{H\text{ on } S_A}$	$\mu_H \frac{S_{O_2}}{K_{O_2} + S_{O_2}} \frac{S_A + S_F}{S_A} \frac{S_A + K_A}{S_A} \frac{S_{NH_4}}{S_{NH_4} + K_{NH_4}} \frac{S_{NO_3}}{S_{NO_3} + K_{NO_3}} \frac{S_{PO_4}}{S_{PO_4} + K_{PO_4}} \frac{S_{ALK}}{S_{ALK} + K_{ALK}} \cdot X_H$
5 Anaerobic hydrolysis of X_{EPS}	$\mu_H \eta_{NO_3, H} \frac{S_{O_2}}{K_{O_2} + S_{O_2}} \frac{S_A + S_F}{S_A} \frac{S_A + K_A}{S_A} \frac{S_{NO_3}}{S_{NO_3} + K_{NO_3}} \frac{S_{NH_4}}{S_{NH_4} + K_{NH_4}} \frac{S_{PO_4}}{S_{PO_4} + K_{PO_4}} \frac{S_{ALK}}{S_{ALK} + K_{ALK}} \cdot X_H$
6 Anoxic hydrolysis of X_{EPS}	$k_{h, EPS} \eta_{f, EPS} \frac{K_{O_2}}{K_{O_2} + S_{O_2}} \frac{S_{NO_3}}{S_{NO_3} + K_{NO_3}} \frac{X_{EPS}/X_H}{X_{EPS}/X_H + K_{EPS}} \cdot X_H$
7 Aerobic hydrolysis of X_{EPS}	$k_{h, EPS} \frac{K_{O_2}}{K_{O_2} + S_{O_2}} \frac{S_{NO_3}}{S_{NO_3} + K_{NO_3}} \frac{X_{EPS}/X_H}{X_{EPS}/X_H + K_{EPS}} \cdot X_H$
8 Aerobic growth of $X_{H\text{ on } S_{MP}}$	$k_{h, EPS} \frac{K_{O_2}}{K_{O_2} + S_{O_2}} \frac{X_{EPS}/X_H}{X_{EPS}/X_H + K_{EPS}} \frac{X_H}{S_{MP}} \cdot X_H$
9 Anoxic growth of $X_{H\text{ on } S_{MP}}$	$\mu_H \eta_{NO_3, H} \frac{S_{O_2}}{K_{O_2} + S_{O_2}} \frac{S_{MP} + K_{SMP}}{S_{MP}} \frac{X_H}{S_{NO_3}} \cdot X_H$
10 Storage of X_{PHA}	$\mu_H \eta_{NO_3, H} \frac{S_{O_2}}{K_{O_2} + S_{O_2}} \frac{S_{NO_3}}{S_{NO_3} + K_{NO_3}} \frac{S_{MP} + K_{SMP}}{S_{MP}} \frac{X_H}{X_{PP}/X_{PAO}} \cdot X_{PAO}$
11 Aerobic Storage of X_{PP}	$q_{PHA} \frac{S_A + K_A}{S_A} \frac{S_{ALK} + K_{ALK}}{S_{ALK}} \frac{K_{PP} + X_{PP}/X_{PAO}}{X_{PP}/X_{PAO}} \cdot X_{PAO}$
12 Anoxic Storage of X_{PP}	$q_{PP} \frac{K_{O_2} + S_{O_2}}{K_{O_2}} \frac{S_{NO_3}}{S_{NO_3} + K_{NO_3}} \frac{K_{ALK} + S_{ALK}}{S_{ALK}} \frac{K_{PHA} + X_{PHA}/X_{PAO}}{X_{PHA}/X_{PAO}} \frac{K_{TTP} + K_{max} - X_{PP}/X_{PAO}}{X_{PHA}/X_{PAO}} \cdot X_{PAO}$
13 Aerobic growth of X_{PAO}	$\eta_{NO_3, H} \frac{S_{O_2}}{K_{O_2}} \frac{S_{NO_3}}{S_{NO_3} + K_{NO_3}} \frac{q_{PP}}{S_{PO_4}} \frac{K_{O_2} + S_{O_2}}{S_{O_2}} \frac{S_{PO_4}}{S_{PO_4} + K_{PO_4}} \frac{K_{ALK} + S_{ALK}}{S_{ALK}} \frac{K_{PHA} + X_{PHA}/X_{PAO}}{X_{PHA}/X_{PAO}} \cdot X_{PAO}$
14 Anoxic growth of X_{PAO}	$\mu_{PAO} \frac{K_{O_2} + S_{O_2}}{K_{O_2}} \frac{S_{NH_4}}{S_{NH_4} + K_{NH_4}} \frac{K_{PO_4} + S_{PO_4}}{S_{PO_4}} \frac{K_{ALK} + S_{ALK}}{S_{ALK}} \frac{K_{PHA} + X_{PHA}/X_{PAO}}{S_{PO_4}} \frac{X_{PHA}/X_{PAO}}{S_{ALK}} \cdot X_{PAO}$
15 Lysis of X_H	$b_H \cdot X_H$
16 Lysis of X_{PAO}	$b_{PAO} X_{PAO} \frac{S_{ALK}}{K_{ALK} + S_{ALK}}$
17 Lysis of X_{AUT}	$b_{AUT} \cdot X_{AUT}$
18 Aerobic growth of X_{AUT}	$\mu_{AUT} \frac{S_{O_2}}{K_{O_2} + S_{O_2}} \frac{S_{NH_4}}{S_{NH_4} + K_{NH_4}} \frac{S_{PO_4}}{K_{PO_4} + S_{PO_4}} \frac{S_{ALK}}{K_{ALK} + S_{ALK}} \cdot X_{AUT}$

five COD: N ratios.

The removal performances of N and P decrease under low COD: N ratios due to the lack of carbon in the A^2O process. Organics in the N and P removal process provide electrons as electron donors, and these organics are removed simultaneously [36]. As can be seen from Fig. 5a, large proportions of organics in the influent were removed in the anaerobic tank, which was the first step in the process. Moreover, the removal rate of COD in the anaerobic tank gradually increased with increasing COD: N ratio. The reason for the decrease of this part COD was because the removal of nutrients in the anaerobic process consumes the organics as electron acceptors [37]. Additionally, the simulation results showed very good prediction fits. Specifically, the maximum and minimum differences are 18.3 % and 0.9 %, respectively, and the average error under five conditions was 7.42 %, indicating that the model was effective.

Based on Fig. 5b, it can be observed that the removal efficiency of S_{NH} is quite low at low COD: N ratio; the removal rate reached only 54.43 %, when COD: N ratio was two. When COD: N is four, the removal rate increases to 72 %, which is consistent with the conclusion that a reduction in the COD: N ratio (i.e., the reduction to four) in the results from Mannina [38] in a significant reduction in N removal. The conversion of ammonia nitrogen to organic N became more difficult when nutrient substances were deficient in microorganisms, due to the scarcity of carbon sources. Unlike low COD: N conditions, the nitrification in the aerobic zone under high COD: N conditions made a significant contribution to S_{NH} removal. The previous dynamic simulation shows that the carbon source had an inhibiting effect on the nitrification of nitrobacteria under high concentrations of organics. It is worth noting that the inhibiting effect is only effective to a certain degree: with the increase of COD: N, the growth rate of the corresponding S_{NH} removal rate slows down. In particular, most of the organics in the A^2O process were removed in the anaerobic zone under high COD: N ratios, presenting a weak inhibition. The increase in COD: N ratio was beneficial to the denitrification process. The concentration of nitrate gradually decreased in the system, which could promote the positive progress of chemical equilibrium, resulting in a high removal efficiency of ammonia

[38]. When COD: N is eight, the removal rate of S_{NH} can reach more than 90 %, which is consistent with the conclusion reported by Lin et al. [39] that found that the average S_{NH} removal rate is higher than 93.2 % when the COD: N ratio is greater than five. Furthermore, there was a small difference between the simulated results and the experimental data for the S_{NH} value. The average error of five conditions was 13.2 %, which indicated that the model was effective in simulating S_{NH} .

As shown in Fig. 5c, the removal efficiency of S_{PO} was unsatisfactory at a low COD: N condition. When COD: N was two, only 1.69 mg/L S_{PO} was released to the anaerobic tank, which was a little higher than the influent. This is because a lot of NO_3 -N goes back to the anaerobic tank, therefore, the nitrate in the returned sludge took precedence over phosphorus-accumulating bacteria to utilize the carbon sources by denitrifying bacteria, which limits PAO growth [40]. Accumulation of volatile fatty acids (VFA) increased with the increase of N in influent water, and VFA is considered to be the best carbon source for PAO [41]. Higher VFA residue can inhibit denitrification and phosphate removal. The fermentation process also interfered with the process of phosphorus release. Compared with the anaerobic phosphorus release process at low COD: N, it was significantly strengthened with a sufficient amount of poly-hydroxyalkanoates (PHA) stored in the phosphorus-accumulating bacteria, when carbon sources were adequate. Meanwhile, a small amount of NO_3 -N in the anoxic region contributes to the effective release of PO_4 -P. The phenomena of denitrifying phosphorus absorption were found in the anoxic zone, where the S_{PO} concentration was lower than that of the influent. At the same time, the S_{PO} absorption mechanism in the aerobic stage also showed different behaviors in the five experimental stages. The amount of S_{PO} absorbed under low COD: N aerobic conditions is lower than under high COD: N conditions, which is consistent with the conclusion of Mannina [38]. Besides, the simulation results were also in line with the real process, and the margin of error was less than 9.18 %.

The concentration curves of SMP and EPS (Fig. 5d & e) show that due to the rapid depletion of organic matter in the anaerobic tank under low influent COD: N, microorganisms are forced to enter the endogenous respiration process early and release a large number of refractory SMP.

Table 3
Stoichiometric matrix for the extended ASM2d-E-M model.

	Process	S_O	S_F	S_A	S_{NO_3}	S_{MP}	X_{EPS}	X_S	X_H	X_I	X_{PAO}	X_{PP}	X_{PHA}	X_{AUT}
1	Aerobic growth of X_H on S_F	$-\frac{1 - f_{S_{MP,H}} - f_{X_{EPS}} - Y_H}{Y_H}$	$\frac{1}{Y_H}$			$\frac{f_{S_{MP,H}}}{Y_H}$	$\frac{f_{X_{EPS}}}{Y_H}$		1					
2	Anoxic growth of X_H on S_F		$\frac{1}{Y_H}$		$-\frac{1 - f_{S_{MP,H}} - f_{X_{EPS}} - Y_H}{2.86Y_H}$	$\frac{f_{S_{MP,H}}}{Y_H}$	$\frac{f_{X_{EPS}}}{Y_H}$		1					
3	Aerobic growth of X_H on S_A	$-\frac{1 - f_{S_{MP,H}} - f_{X_{EPS}} - Y_H}{Y_H}$		$\frac{1}{Y_H}$		$\frac{f_{S_{MP,H}}}{Y_H}$	$\frac{f_{X_{EPS}}}{Y_H}$		1					
4	Anoxic growth of X_H on S_A			$\frac{1}{Y_H}$	$-\frac{1 - f_{S_{MP,H}} - f_{X_{EPS}} - Y_H}{2.86Y_H}$	$\frac{f_{S_{MP,H}}}{Y_H}$	$\frac{f_{X_{EPS}}}{Y_H}$		1					
5	Anaerobic hydrolysis of X_{EPS}		f_{S_F}			$1 - f_{S_F}$	-1							
6	Anoxic hydrolysis of X_{EPS}		f_{S_F}			$1 - f_{S_F}$	-1							
7	Aerobic hydrolysis of X_{EPS}		f_{S_F}			$1 - f_{S_F}$	-1							
8	Aerobic growth of X_H on S_{MP}	$-\frac{1 - Y_{S_{MP,H}}}{Y_{S_{MP,H}}}$			$-\frac{1 - Y_{S_{MP,H}}}{2.86Y_{S_{MP,H}}}$	$-\frac{1}{Y_{S_{MP,H}}}$			1					
9	Anoxic growth of X_H on S_{MP}					$-\frac{1}{Y_{S_{MP,H}}}$			1					
10	Storage of X_{PHA}			-1								$-Y_{PO_4}$	1	
11	Aerobic Storage of X_{PP}	$-Y_{PHA}$					$f_{PP,EPS}$					$1 - f_{PP,EPS}$	$-Y_{PHA}$	
12	Anoxic Storage of X_{PP}				Y_{PHA}		$f_{PP,EPS}$					$1 - f_{PP,EPS}$	$-Y_{PHA}$	
13	Aerobic growth of X_{PAO}	$-\frac{1 - f_{S_{MP,P}} - f_{X_{EPS}} - Y_H}{Y_H}$				$\frac{f_{S_{MP,P}}}{Y_H}$	$\frac{f_{X_{EPS}}}{Y_H}$				1			$\frac{1}{Y_H}$
14	Anoxic growth of X_{PAO}				$-\frac{1 - f_{S_{MP,P}} - f_{X_{EPS}} - Y_H}{2.86Y_H}$	$\frac{f_{S_{MP,P}}}{Y_H}$	$\frac{f_{X_{EPS}}}{Y_H}$				1			$\frac{1}{Y_H}$
15	Lysis of X_H					$f_{S_{MP,L}}$		$1 - f_{S_{MP,L}} - f_{X_I}$	-1	f_{X_I}				
16	Lysis of X_{PAO}					$f_{S_{MP,L}}$		$1 - f_{S_{MP,L}} - f_{X_I}$		f_{X_I}	-1			
17	Lysis of X_{AUT}					$f_{S_{MP,L}}$		$1 - f_{S_{MP,L}} - f_{X_I}$		f_{X_I}				-1
18	Aerobic growth of X_{AUT}	$-\frac{4.75 - f_{S_{MP,A}} - f_{X_{EPS}} - Y_A}{Y_A}$			$\frac{1}{Y_A}$	$-\frac{f_{S_{MP,A}}}{Y_A}$	$-\frac{f_{X_{EPS}}}{Y_A}$							1

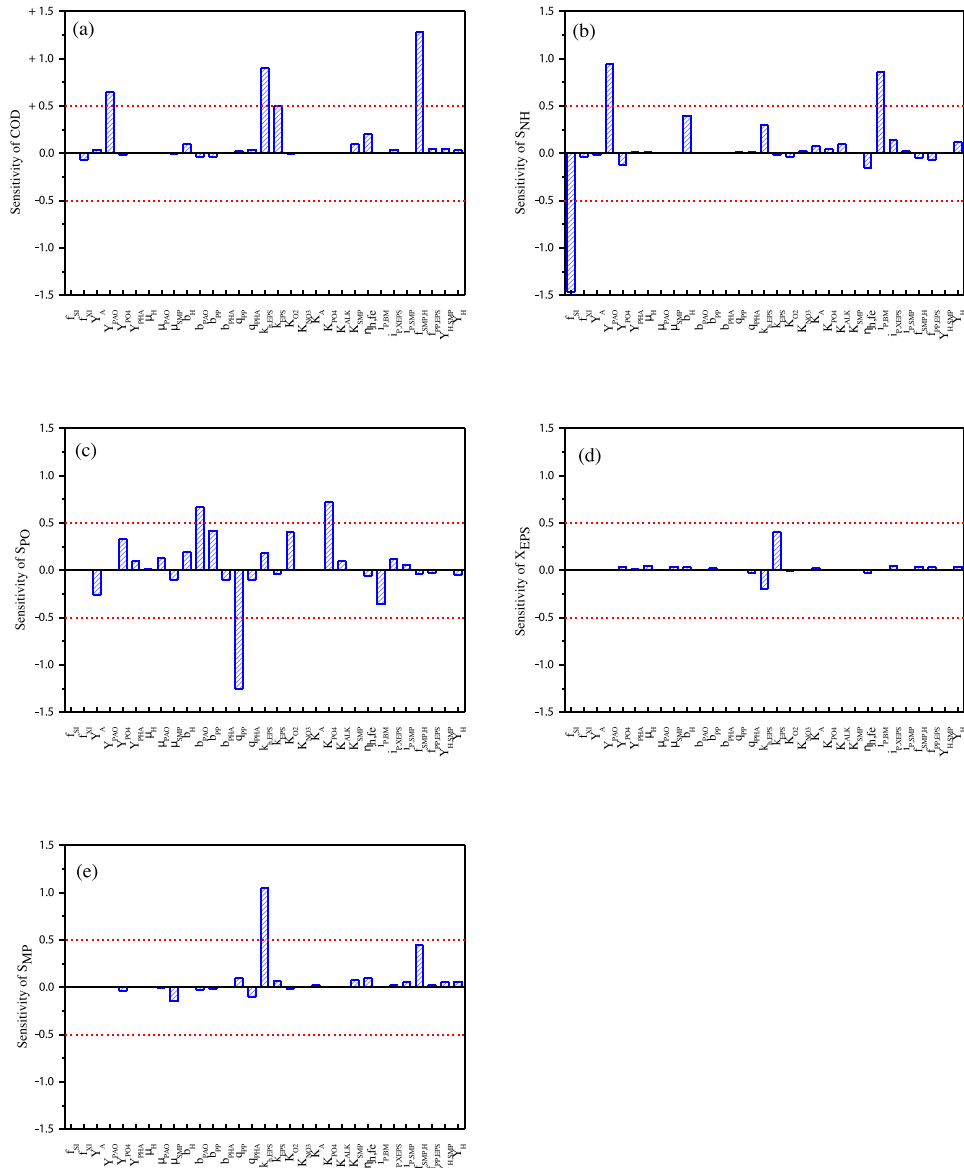


Fig. 3. Sensitivity analysis of the ASM2d-E-M model parameters on the model outputs: (a) COD, (b) S_{NH_4} , (c) S_{PO_4} , (d) X_{EPS} , (e) S_{MP} .

Moreover, as the degradation of SMP components produced by endogenous respiration process is slower than that produced by the substrate utilization process, there is an increase in SMP concentration and the slow anaerobic hydrolysis of EPS, which decreases the total EPS. After the anaerobic stage, the substrate is rapidly consumed and the total EPS amount increases. The formation of EPS mainly occurs during substrate consumption and it is cleaved to SMP when the substrate is restricted. Therefore, it was observed that the total EPS decreased slightly in the modeling and experimental results due to the hydrolysis or decay of EPS in the aerobic tank. Under high COD: N, due to the existence of a large number of organic substances in the system and the low concentration of SMP, the majority of microbial activity is degrading fermentable, readily biodegradable organic substrates (S_F). Along with the further consumption of S_F , the microbial degradation rate of SMP increases gradually. In the aerobic tank, due to the large consumption of S_F in the anaerobic tank and anoxic tank, the main microbial activity is SMP metabolism, while the biodegradability of SMP is lower than that of S_F , resulting in the net accumulation of SMP in the system. The SMPs produced in the process of oxidizing carbon sources can be used by microorganisms for growth and metabolism, resulting in greater hydrolyzation of EPS.

3.4.2. Model application

The purpose of this section is to verify the ASM2d-E-M model, by comparing the simulations and the practical measurements of a 150-day lab-scale A^2O under different COD: N conditions. Fig. 6 shows the results predicted by the ASM2d-E-M model and the measured results of effluent COD, S_{NH_4} , S_{PO_4} , SMP, and EPS concentration profiles in the A^2O system.

As shown in Fig. 6a, according to the results of the effluent concentration, the system presented favorable COD removal under both low COD: N and high COD: N conditions. This indicates that the COD: N ratio has little effect on COD removal. This is consistent with the conclusion of Lin [39], and is attributed to good bioactivity within the system, and the biological adaptability of the wastewater characteristics. This suggests that the C: N ratio has little effect on the removal of COD because in this study, synthetic substrates were used that are easily biodegradable (i.e., glucose). The COD trend predicted by the model is the same as that predicted by the E-ASM1 [42], which gradually decreases with the increase of COD: N ratio from 4:1 to 20:1.

Regarding the concentration curves of SMP and EPS, when COD: N was 2:1, the EPS average value was more than 1.28, 1.44, 1.65, and 2.31 times of the corresponding value when COD: N was 4, 8, 12, and 16, respectively. At the lowest COD: N ratio, EPS and SMP content in the

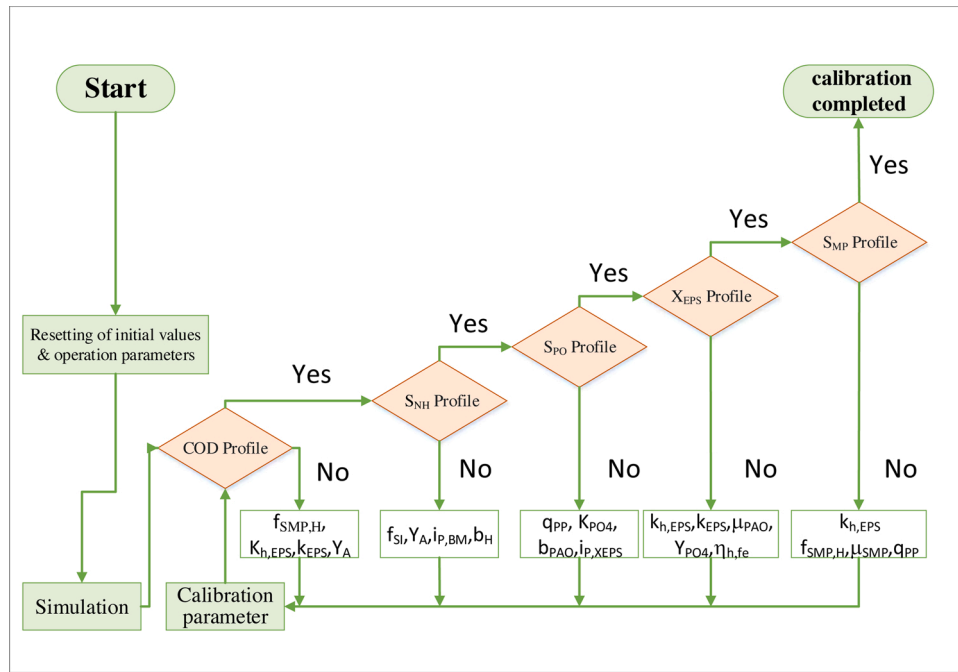


Fig. 4. Specific calibration steps for ASM2d-E-M.

Table 4

Stoichiometric and kinetic model calibrated parameters for the the ASM2d-E-M model.

Symbol	Default value	Calibration value	Reported	Reference
$f_{SMP,H}$	0.0963	0.08	–	Fit
Y_{PAO}	0.625	0.61	0.625	ASM2d
$i_{P,BM}$	0.02	0.024	0.02	ASM2d
q_{PP}	1.50	1.7	1.50	ASM2d
K_{PO_4}	0.01	0.012	0.01	ASM2d
b_{PAO}	0.2	0.18	0.1–0.25	(Cosenza et al. [25])
μ_{PAO}	1.00	1.02	1.00	ASM2d
$k_{h,EPS}$	0.0071	0.0075	0.0071	(Ni and Zeng [6])
μ_{SMP}	0.0029	0.003	0.0029	(Ni and Zeng [6]; Yang et al. [20])

A^2O system were the highest. These results indicate that the lowest COD: N value promotes the suspension and biofilm biomasses [43]. Under influent COD: N conditions, a large amount of by-products, or SMPs, were generated by sludge due to the sufficient organic sources. These organics were more biodegradable than those produced during endogenous respiration [14]. The results from the model simulation were consistent with the laboratory results. The average error of five conditions with EPS was lower than 1.50 %, and with SMP it was lower than 2.59 %.

As shown in Fig. 6b, the S_{NH} concentration is contrary to the trend predicted by E-ASM1 (Gao et al. [42]), which may be because in this study, when changing the COD: N, the carbon content was fixed while the nitrogen content was changed. Under the condition of constant carbon source, the carbon oxidation and denitrification of heterotrophic bacteria cannot be carried out normally, due to the low concentration of COD and the high concentration of ammonia nitrogen in the influent. This explains why the S_{NH} content in effluent is higher when COD: N is lower.

Average S_{PO} decreases with the increase of the COD: N ratio from 2:1 to 12:1, but it increases when COD: N increases to 16:1. This may be due to the P: the increase in carbon strengthens the phosphorus removal

process. Phosphorus-accumulating bacteria store enough carbon for the excessive phosphorus absorption that occurs in the subsequent aerobic process; however, the phosphorus absorption process not only occurs in the aerobic section, but also in the anoxic section. Denitrifying phosphorus-accumulating bacteria use nitrate nitrogen as an electron acceptor and organic matter as an electron donor. However, under high COD: N, the amount of organics adsorbed on the sludge surface increases. Denitrifying bacteria will preferentially use the organics adsorbed on the surface for denitrification in the anoxic stage, which consumes a large amount of nitrate nitrogen; therefore, the phosphorus absorption in the environment is not sufficient, as nitrate nitrogen used for denitrifying phosphorus absorption is deficient.

The consistency between the model output and experimental data supports the utility of the ASM2d-E-M model in representing the components and their formation/consumption.

3.5. Challenges and future perspectives of A^2O process

The contradiction between the high-energy needs of humans, and the limited available resources worldwide, has led to greater attention to the recycling of nutrients, energy, water, heavy metals, alkalis, acids, bioelectricity, and biofuels from wastewater. The ability to recover these resources could make wastewater itself a valuable resource in the future. Improved technologies are effective tools to help treat wastewater and recycle resources. Establishing links between A^2O new technologies, and the recycling of nutrients and energy from wastewater is a challenge. The extended ASM2d-E-M model has good generality in representing the composition of wastewater and its formation/consumption, which can provide an effective reference for the mathematical simulation of BNR. When running at low C: N ratios, the use of the extended ASM2d-E-M is expected to provide optimal strategies for enhancing BNR processes, such as phosphorus removal, adding external carbon sources, or nitrate recovery adjustment, to effectively treat wastewater, save energy, and recycle resources.

4. Conclusion

This work explored the extended ASM2d-E-M model for tracking the effluent concentrations in the BNR system. The A^2O reactor, with an

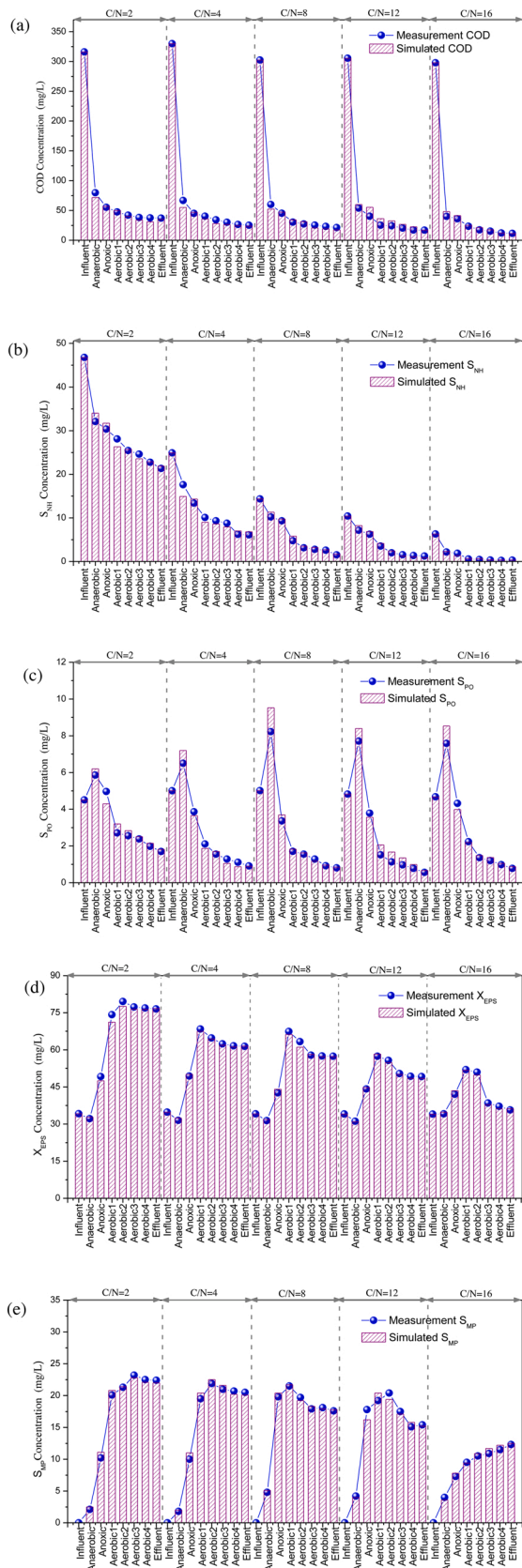


Fig. 5. Model verifications and simulations of the experimental results for an A2O reactor of biological nutrient removal with ASM2d-E-M: (a) COD concentration; (b) S_{NH} concentration; (c) S_{PO} concentration; (d) X_{EPS} concentration; (e) S_{MP} concentration.

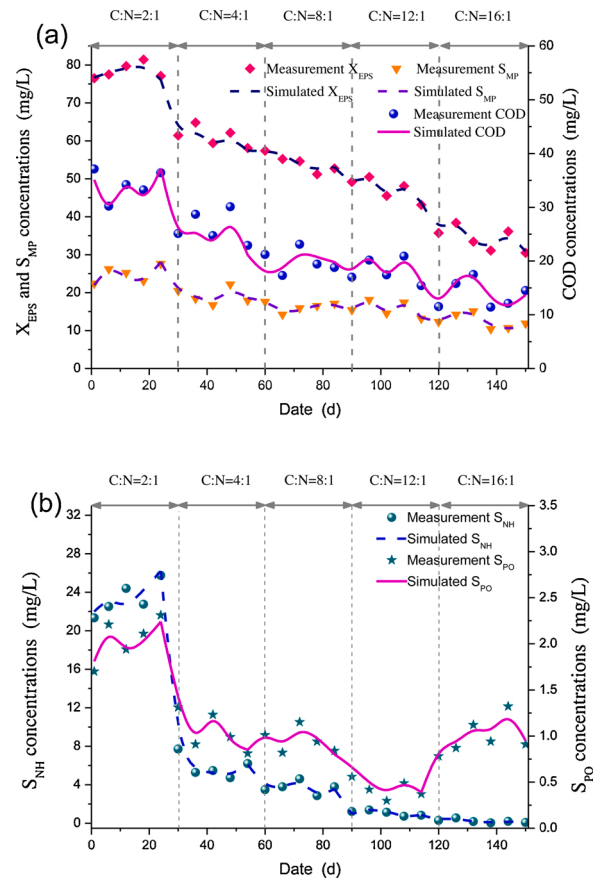


Fig. 6. The dynamic simulation results of ASM2d-SMP-EPS for an A²O reactor (a) COD, S_{MP} and X_{EPS} concentration; (b) S_{NH} and S_{PO} concentration.

insufficient influent COD: N ratio during running was characterized. The extended unified model successfully integrated the unified model of active and inert biomass in activated sludge, as well as EPS and SMP. This model had the advantage of quantifying the influence of the influent COD: N ratio in the A²O on substrate hydrolysis and the formation of SMP and EPS. The sensitivity of the model was analyzed by the local sensitivity analysis method, and nine important model parameters were selected that greatly reduced the number of to-be-calibrated model parameters. The model parameters were calibrated in a stepwise manner. Independent experimental results, using a laboratory-scale A²O under steady-state conditions, successfully verified the ASM2d-E-M model. The good consistency between the model output and the measured value of the parallel experimental study on the laboratory-scale A²O reactor showed that the ASM2d-E-M model could successfully be used to design and optimize such systems, with different influent COD: N ratios. The ASM2d-E-M model was used to predict the impact of different influent COD: N ratios on COD, S_{NH} , S_{PO} , EPS, and SMP concentrations. Model simulations showed that at low COD: N ratios, nitrogen and phosphorus removal efficiencies decreased due to the lack of a carbon source. According to the final effluent, the system presented favorable COD removal efficiency under low COD: N and high COD: N conditions. However, the removals of S_{NH} and S_{PO} were not good at low COD: N ratios. In general, the ASM2d-E-M successfully established in this study provides a useful reference for the mathematical simulation and effective operation of actual industrial wastewater treatment plants under a low COD: N ratio.

Declaration of Competing Interest

The authors declare that they have no known competing financial interests or personal relationships that could have appeared to influence

the work reported in this paper.

Acknowledgements

The research was jointly supported by the Nanqi Ren Studio, Academy of Environment & Ecology, Harbin Institute of Technology (Grant No. HSCJ201702), the National Science Foundation of China (No. 52070058), the National Research Council of Science and Technology Major Project of Twelfth Five Years (Grant No. 2014ZX07201-012-2), Open Project of State Key Laboratory of Urban Water Resource and Environment, Harbin Institute of Technology (No. ES201810-02), Natural Science Foundation of Heilongjiang Province (YQ2020E020), Special support from China postdoctoral fund (2018T110303); and Special support from Heilongjiang Postdoctoral Found (LBH-TZ14).

References

- [1] H. Hu, K. Liao, W. Xie, J. Wang, B. Wu, H. Ren, Modeling the formation of microorganism-derived dissolved organic nitrogen (mDON) in the activated sludge system, *Water Res.* 174 (2020), 115604.
- [2] F. Gao, J. Nan, X. Zhang, T. Wu, A dynamic modelling of nutrient metabolism in a cyclic activated sludge technology (CAST) for treating low carbon source wastewater, *Environ. Sci. Pollut. Res. Int.* 24 (20) (2017) 17016–17030.
- [3] D. Mulkerrins, C. Jordan, S. McMahon, E. Collieran, Evaluation of the parameters affecting nitrogen and phosphorus removal in anaerobic/anoxic/oxic (A/A/O) biological nutrient removal systems, *J. Chem. Technol. Biotechnol.* 75 (4) (2000) 261–268.
- [4] F. Fang, L.-L. Qiao, J.-S. Cao, Y. Li, W.-M. Xie, G.-P. Sheng, H.-Q. Yu, Quantitative evaluation of A2O and reversed A2O processes for biological municipal wastewater treatment using a projection pursuit method, *Sep. Purif. Technol.* 166 (2016) 164–170.
- [5] Y. Ma, Y.-z. Peng, X.-l. Wang, S.-y. Wang, Nutrient removal performance of an anaerobic-anoxic-aerobic process as a function of influent C/P ratio, *J. Chem. Technol. Biotechnol.* 80 (10) (2005) 1118–1124.
- [6] B.-J. Ni, R.J. Zeng, A novel approach to evaluate the production kinetics of extracellular polymeric substances (EPS) by activated sludge using weighted nonlinear least-squares analysis, *Environ. Sci. Technol.* 43 (2009) 3743–3750.
- [7] T.T. Lee, F.Y. Wang, R.B. Newell, On the modelling and simulation of a BNR activated sludge process based on distributed parameter approach, *Water Sci. Technol.* 39 (6) (1999) 79–88.
- [8] R. Carrette, D. Bixio, C. Thoeye, P. Ockier, Full-scale application of the IAWQ ASM No.2D model, *Water Sci. Technol.* 44 (2–3) (2001) 17–24.
- [9] A. Fenu, G. Guglielmi, Activated sludge model (ASM) based modelling of membrane bioreactor (MBR) processes: a critical review with special regard to MBR specificities, *Water Res.* 44 (2010) 4272–4294.
- [10] F. Gao, J. Nan, X. Zhang, Simulating a cyclic activated sludge system by employing a modified ASM3 model for wastewater treatment, *Bioprocess Biosyst. Eng.* 40 (6) (2017) 877–890.
- [11] M. Henze, W. Gujer, T. Mino, T. Matsuo, M.C. Wentzel, Gv.R. Marais, Activated sludge model No.2d, ASM2d, *Water Sci. Technol.* 39 (1) (1999) 165–182.
- [12] T. Jiang, S. Myngher, Modelling the production and degradation of soluble microbial products (SMP) in membrane bioreactors (MBR), *Water Res.* 42 (2008) 4955–4964.
- [13] D.J. Barker, D.C. Stuckey, A review of soluble microbial products (SMP) in wastewater treatment systems, *Water Res.* 33 (14) (1999) 3063–3082.
- [14] T. Janus, B. Ulanicki, Modelling SMP and EPS formation and degradation kinetics with an extended ASM3 model, *Desalination* 261 (1–2) (2010) 117–125.
- [15] S.G. Lu, T. Imai, M. Ukita, M. Sekine, T. Higuchi, M. Fukagawa, A model for membrane bioreactor process based on the concept of formation and degradation of soluble microbial products, *Water Res.* 35 (8) (2001) 2038–2048.
- [16] W.-M. Xie, B.-J. Ni, T. Seviour, G.-P. Sheng, H.-Q. Yu, Characterization of autotrophic and heterotrophic soluble microbial product (SMP) fractions from activated sludge, *Water Res.* 46 (19) (2012) 6210–6217.
- [17] B.J. Ni, B.E. Rittmann, F. Fang, J. Xu, H.Q. Yu, Long-term formation of microbial products in a sequencing batch reactor, *Water Res.* 44 (13) (2010) 3787–3796.
- [18] S.M. Libelli, P. Ratini, A. Spagni, G. Bortone, Implementation, study and calibration of a modified ASM2d for the simulation of SBR processes, *Water Res.* 35 (3) (2001) 69–76.
- [19] C.S.L.B.E. Rittmann, A unified theory for extracellular polymeric substances, soluble microbial products, and active and inert biomass, *Water Res.* 36 (11) (2002) 2711–2720.
- [20] S.S. Yang, W. Guo, Y. Chen, S. Peng, J. Du, H. Zheng, X. Feng, N. Ren, Simultaneous in-situ sludge reduction and nutrient removal in an A 2 MO-M system: performances, mechanisms, and modeling with an extended ASM2d model, *Water Res.* 88 (2016) 524–537.
- [21] S.S. Yang, J.W. Pang, W.Q. Guo, X.Y. Yang, Z.Y. Wu, N.Q. Ren, Z.Q. Zhao, Biological phosphorus removal in an extended ASM2 model: roles of extracellular polymeric substances and kinetic modeling, *Bioresour. Technol.* 232 (2017) 412–416.
- [22] S.H. Jenkins, Standard methods for the examination of water and wastewater, *Water Res.* 16 (10) (1982) 1495–1496.
- [23] Michel DuBois, K.A. Gilles, J.K. Hamilton, P.A. Rebers, Fred Smith, Colorimetric method for determination of sugars and related substances, *Anal. Chim. Acta* 28 (1956) 350–356.
- [24] O.H. Lowry, N.J. Rosebrough, A.L. Farr, R.J. Randall, Protein measurement with the Folin phenol reagent, *J. Biol. Chem.* 193 (1951) 265–275.
- [25] A. Cosenza, G. Mannina, P.A. Vanrolleghem, M.B. Neumann, Global sensitivity analysis in wastewater applications: a comprehensive comparison of different methods, *Environ. Model. Softw.* 49 (2013) 40–52.
- [26] M. Henze, W. Gujer, T. Mino, Mv. Loosdrecht, Activated Sludge Models ASM1, ASM2, ASM2D and ASM3, 2000.
- [27] X. Lu, T.D.S. Pereira, H.E. Al-Hazmi, J. Majtacz, Q. Zhou, L. Xie, J. Makinia, Model-based evaluation of N2O production pathways in the anammox-enriched granular sludge cultivated in a sequencing batch reactor, *Environ. Sci. Technol.* 52 (5) (2018) 2800–2809.
- [28] T. Jiang, X. Liu, M.D. Kennedy, J.C. Schippers, P.A. Vanrolleghem, Calibrating a side-stream membrane bioreactor using Activated Sludge Model No. 1, *Water Sci. Technol.* 52 (2005) 359–367.
- [29] A. Cosenza, G. Mannina, P.A. Vanrolleghem, M.B. Neumann, Variance-based sensitivity analysis for wastewater treatment plant modelling, *Sci. Total Environ.* 470–471 (2014) 1068–1077.
- [30] G. Mannina, A. Cosenza, G. Viviani, G.A. Ekama, Sensitivity and uncertainty analysis of an integrated ASM2d MBR model for wastewater treatment, *Chem. Eng. J.* 351 (2018) 579–588.
- [31] R. Brun, M. Kühni, H. Siegrist, W. Gujer, P. Reichert, Practical identifiability of ASM2d parameters—systematic selection and tuning of parameter subsets, *Water Res.* 36 (16) (2002) 4113–4127.
- [32] W. Gujer, M. Henze, T. Mino, T. Matsuo, The activated sludge model NO.2: biological phosphorus remove, *Water Sci. Technol.* 31 (1995) 1–15.
- [33] M. Henze, G. C.P.L. Jr., W. Gujer, Gv.R. Marais, T. Matsuo, Activated Sludge Model No. 1, by IAWPRC Task Group on Mathematical Modelling for Design and Operation of Biological Wastewater Treatment, 1987, pp. 1–33.
- [34] F. García-Usach, J. Ribes, J. Ferrer, A. Seco, Calibration of denitrifying activity of polyphosphate accumulating organisms in an extended ASM2d model, *Water Res.* 44 (18) (2010) 5284–5297.
- [35] G. Insel, G. Sin, D.S. Lee, I. Nopens, P.A. Vanrolleghem, A calibration methodology and model-based systems analysis for SBRs removing nutrients under limited aeration conditions, *J. Chem. Technol. Biotechnol.* 81 (4) (2006) 679–687.
- [36] S. Ge, Y. Peng, S. Wang, J. Guo, B. Ma, L. Zhang, X. Cao, Enhanced nutrient removal in a modified step feed process treating municipal wastewater with different inflow distribution ratios and nutrient ratios, *Bioresour. Technol.* 101 (23) (2010) 9012–9019.
- [37] H.Y. Chang, C.F. Ouyang, Improvement of nitrogen and phosphorus removal in the anaerobic-oxic-anoxic-OXIC (AOAO) process by stepwise feeding, *Water Sci. Technol.* 42 (3–4) (2000) 89–94.
- [38] G. Mannina, M. Capodici, A. Cosenza, D. Di Trapani, aCarbon and nutrient biological removal in a University of Cape Town membrane bioreactor: analysis of a pilot plant operated under two different C/N ratios, *Chem. Eng. J.* 296 (2016) 289–299.
- [39] J. Lin, P. Zhang, G. Li, J. Yin, J. Li, X. Zhao, Effect of COD/N ratio on nitrogen removal in a membrane-aerated biofilm reactor, *Int. Biodeterior. Biodegradation* 113 (2016) 74–79.
- [40] R.A. Hamza, M.S. Zaghoul, O.T. Iorhemen, Z. Sheng, J.H. Tay, Optimization of organics to nutrients (COD:N:P) ratio for aerobic granular sludge treating high-strength organic wastewater, *Sci. Total Environ.* 650 (Pt 2) (2019) 3168–3179.
- [41] R.R. Singhanina, A.K. Patel, G. Christophe, P. Fontanille, C. Larroche, Biological upgrading of volatile fatty acids, key intermediates for the valorization of biowaste through dark anaerobic fermentation, *Bioresour. Technol.* 145 (2013) 166–174.
- [42] F. Gao, J. Nan, S. Li, Y. Wang, Modeling and simulation of a biological process for treating different COD:N ratio wastewater using an extended ASM1 model, *Chem. Eng. J.* 332 (2018) 671–681.
- [43] G. Mannina, G.A. Ekama, M. Capodici, A. Cosenza, D. Di Trapani, H. Ødegaard, Moving bed membrane bioreactors for carbon and nutrient removal: the effect of C/N variation, *Biochem. Eng. J.* 125 (2017) 31–40.
- [44] C.E. Laspidou, B.E. Rittmann, Non-steady state modeling of extracellular polymeric substances, soluble microbial products, and active and inert biomass, *Water Res.* 36 (8) (2002) 1983–1992.